TP53 or CDKN2A/B covariation in ALK/RET/ROS1-rearranged NSCLC is associated with a high TMB, tumor immunosuppressive microenvironment and poor prognosis

Bin Jiang
Guiqian International General Hospital
Liwen Hu
Zhongnan Hospital of Wuhan University
Daling Dong
Guiqian International General Hospital
Zixin Guo
Zhongnan Hospital of Wuhan University
Wei Wei
Guiqian International General Hospital
Chao Wang
Guiqian International General Hospital
Weikang Shao
Genecast Biotechnology Co., Ltd
Ting Ma
Genecast Biotechnology Co., Ltd
Yanhui Chen
Genecast Biotechnology Co., Ltd
Qingyun Li
Genecast Biotechnology Co., Ltd
Weidong Hu (huwd@whu.edu.cn)
Zhongnan Hospital of Wuhan University

Research Article

Keywords: occurring, Tumor microenvironment, TMB, Non-small cell lung cancer, Immunotherapy

Posted Date: April 24th, 2023

DOI: https://doi.org/10.21203/rs.3.rs-2837365/v1

Additional Declarations: Competing interest reported. The authors declared the following potential conflicts of interest with respect to the research, authorship, and/or publication of this article: Weikang Shao, Ting Ma, Yanhui Chen and Qingyun Li are employees of Genecast Biotechnology Co., Ltd. The other authors declare that they have no competing interests.

Version of Record: A version of this preprint was published at Journal of Cancer Research and Clinical Oncology on June 1st, 2023. See the published version at https://doi.org/10.1007/s00432-023-04924-7.

Abstract

Introduction: ALK-rearranged lung adenocarcinomas with TP53 mutations have more unstable genomic features, poorer ALK-TKI efficacy and a worse prognosis than ALK-rearranged lung adenocarcinomas with wild-type TP53. Here, we examine the gene variations that co-occur with ALK/RET/ROS1 rearrangements in NSCLC and the corresponding tumor immune microenvironment, as well as their association with prognosis.

Methods: A total of 155 patients with ALK/RET/ROS1 fusions were included retrospectively. Tumor genome mutation analysis was performed by next-generation sequencing. PD-L1 expression and tumor-infiltrating lymphocytes were assessed by multiplex immunohistochemistry. The correlations among gene covariation, the tumor immune microenvironment, and clinicopathological characteristics were analyzed.

Results: Among the 155 patients, concomitant TP53 mutation appeared most frequently (31%), followed by CDKN2A/B copy number loss (15%). The ALK/RET/ROS1 fusion and TP53 or CDKN2A/B covariation group had more males and patients with stage IV disease ($p<0.001$, $p=0.0066$). Patients with TP53 or CDKN2A/B co-occurrence had higher tumor mutation burdens and more neoantigens ($p<0.001$, $p=0.0032$). PD-L1 expression was higher in the tumor areas of the TP53 or CDKN2A/B co-occurring group ($p=0.00038$). However, the levels of $CD8^+$, $CD8^+PD1^-$, and $CD8^+PD\text{-}L1^-$ TILs were lower in the tumor areas of this group ($p=0.043$, $p=0.029$, $p=0.025$). In the TCGA NSCLC cohorts, the top 2 mutated genes were CDKN2A/B (24%) and TP53 (16%). The TP53 or CDKN2A/B co-occurring group had higher tumor mutation burdens and shorter OS ($p<0.001$, $p<0.001$).

Conclusions: Patients with co-occurring TP53/CDKN2A/B variations and ALK/RET/ROS1 rearrangements are associated with high TMB, more neoantigens, an immunosuppressive microenvironment and a worse prognosis.

Background

With the development of next-generation sequencing technologies, ALK/RET/ROS1 rearrangements are being detected more frequently than before, and more clinically significant comutations have been identified in lung cancer. ALK-positive lung cancer accounts for approximately 3–7% of non-small cell lung cancer (NSCLC) cases.[1,2] ROS1 and RET gene rearrangements account for approximately 1–2% of all NSCLC cases.[3–5] Patients with ALK-rearranged NSCLC have similar clinical features to patients with ROS1-rearranged NSCLC; for example, they are often young and nonsmokers and have adenocarcinoma, which suggests that ALK and ROS1 rearrangements may have a similar pathogenesis.[3] ALK-specific tyrosine kinase inhibitors (TKIs) have consistently shown superior efficacy and tolerability in patients with ALK-positive lung cancer.[1,2] However, the degree of benefit of ALK-TKIs varied among different ALK-positive patients. Although such heterogeneity lacks accepted reasons, genomic co-occurrence is thought to affect the efficacy of ALK-TKIs.[6] Several studies have demonstrated that the co-occurrence of TP53

mutation and ALK rearrangement is a poor prognostic factor, resulting in shorter progression-free survival (PFS) and overall survival (OS).[7]

Some studies on gene fusions and comutations in lung cancer have analyzed the relationship between PD-L1 expression and comutation, trying to explore the poor prognosis of comutated patients from the perspective of the tumor immune microenvironment. PD-L1 is highly expressed in NSCLC with both gene fusion and mutation, and previous studies have attempted to explain this phenomenon. It could be that ALK upregulates PD-L1 via HIF-1α and/or STAT3-derived pADC or that ALK and mutant EGFR upregulate the expression by activating the PI3K-AKT and MEK-ERK signaling pathways in NSCLC.[8,9] However, in NSCLC with co-occurring EGFR mutation and ALK rearrangement, tumors were rarely accompanied by $CD8^+$ tumor-infiltrating lymphocyte (TIL) infiltration and PD-L1 expression. This may explain the low response rate to PD-1/PD-L1 inhibitors in this group of patients.[10] However, the sample size of these studies was small, and the types of TILs in the tumor microenvironment studied were limited to one or two, so a larger sample size and more types of TILs are needed for further study.

This study focuses on describing the co-occurring gene mutations and the corresponding TIL infiltration in ALK/RET/ROS1-rearranged NSCLC to provide a clear subclassification and a complete picture of the overall tumor immunogenicity and immune microenvironment. The tumor immune microenvironment (TIME) was assessed by the levels of multiple markers, including PD-1, PD-L1, CD8, and CD68. A deeper exploration of co-occurring genes in NSCLC can strengthen the selection of patients for more precise treatment and guide the development of new treatment strategies.

Materials And Methods

Patients and samples

A total of 155 tumor tissue samples from NSCLC patients harboring ALK/RET/ROS1 rearrangements were retrospectively collected from Zhongnan Hospital of Wuhan University and Guiqian International General Hospital, all of which were either surgical specimens or puncture specimens at the time of primary treatment. Paired samples were taken from the same patient. Tumor tissue was collected along with para-carcinoma tissue or blood samples as a control. The study design was approved by the Ethics Committees of Zhongnan Hospital of Wuhan University and Guiqian International General Hospital. The validation cohort contained 340 samples with both RNA transcriptome and DNA mutation data, which were selected from the lung adenocarcinoma (LUAD) and lung squamous cell carcinoma (LUSC) categories in The Cancer Genome Atlas (TCGA, https://portal.gdc.cancer.gov/).

DNA extraction and capture-based targeted DNA sequencing

DNA was extracted from 5 ~ 10 μm formalin-fixed paraffin-embedded (FFPE) sections. Hybrid capture-based comprehensive genomic profiling analysis identified genetic rearrangement events and co-

occurring genomic alterations (GAs). DNA libraries were captured with a personalized customization panel of 769 genes (Genecast, Beijing, China), which comprehensively covered sensitive and resistant sites and immunotherapy-related molecular markers. After library construction, the target region was captured by probe hybridization, and the enriched target region was paired-end sequenced using an Illumina NovaSeq 6000 sequencing platform.

Bioinformatics analysis pipeline

Once the raw sequencing data were obtained, the data were subjected to a comprehensive series of bioinformatic analyses. Quality control was first performed using Trimmomatic (v0.36), and data that passed quality control were analyzed downstream. For data mapping, reference alignment was performed via BWA aligner (v0.7.17) and Picard (v2.23.0) for sorting and duplication masking. Then, Genome Analysis Toolkit (GATK, version 3.7) was used for realignment. VarDict (version 1.5.1) was used for the variant calling step to call single-nucleotide variant (SNV) mutations, and gene functions were annotated with ANNOVAR. SNVs were filtered with the following rules: (i) The loci with a sequencing depth of less than 30x were filtered out. (ii) Mutations in the blacklist were filtered out, while those in the whitelist were retained. (iii) SNV mutations in the intronic or intergenic regions and nonsense mutations were filtered out. Copy number variations (CNVs) were called via Cnvkit (v0.9.2) from the tumor samples, and the Genecast normal database was used as a paired control. The copy number threshold for CNV gain was four, and that for CNV loss was 1.2. The tumor mutational burden (TMB) test used a standard protocol, while the analysis method involved a proprietary module from the Genecast company. To determine the TMB value, the numbers of somatic nonsynonymous SNVs detected by next-generation sequencing (NGS) were quantified, and the values were extrapolated to the whole exome using a validated algorithm. First, somatic SNV mutations were screened to identify candidate loci for calculating the TMB value. The standards for filtering nonsynonymous mutations in the coding region were as follows. (i) Mutations in driver genes and hotspot mutations included in the Exome Aggregation Consortium (ExAC)/COSMIC database were filtered out. (ii) Mutation loci that met certain sequencing depth and mutation frequency thresholds were identified. Second, TMB was calculated based on the candidate mutations for the tumor mutation load screened above, equal to the absolute number of mutation counts divided by the panel's base number of exonic regions. It was measured in mutations per Mb. ALK/RET/ROS1 rearrangements status were also identified by analysis of NGS.

Fluorescent multiplex immunohistochemistry (mIHC) analysis

Tissue samples were processed into paraffin-embedded blocks and then cut into 3–5 μm FFPE sections. The immune markers, including CD68, CD8, PD-L1, and PD-1, were identified and quantified by mIHC. Then, the infiltration of $CD8^+$ TILs, $CD68^+$ macrophages, $CD8^+PD\text{-}1^+$ TILs, and $CD68^+PD\text{-}L1^+$ macrophages was evaluated. Samples of immunohistochemical markers were evaluated with antibodies. In this case, the main antibodies used were CD8 antibody (clone 144B, ab17147, Abcam; dilution 1:25), CD68 antibody (clone KP1, ZM-0060, Zsbio; dilution 1:400), CD163 antibody (clone 10D6, ZM0428, Zsbio; dilution 1:200), PD-L1 antibody (clone SP142, Ventana; dilution 1:25), and PD-1 antibody (clone CAL20,

ab237728, Abcam; dilution 1:100). Each antigen was subjected to a complete labeling process, including primary antibody incubation, secondary antibody incubation, and TSA visualization, before the next antibody was labeled. To better assess the expression of immune markers quantitatively, the percentage of positive cells was used to describe the fluorescent staining result, and it was interpreted by capturing images of the tumor area at 200x magnification and using image analysis software for quantitative statistical analysis. The fluorescent result is the percentage of positive staining of total nucleated cells. All the mIHC slides were scanned by the PerkinElmer Vectra (Vectra 3.0.5; PerkinElmer, Massachusetts, USA) platform. In addition, PD-L1 was also stained with traditional diaminobenzidine (DAB), and the staining results were used as a reference and for quality control.

Statistical analysis

Statistical analysis was performed using the R software program (version 3.6.1, https://www.r-project.org/). The Wilcoxon test was used to compare whether there was a significant difference in the TIME between the co-occurring and control groups. Wilcoxon rank-sum or Kruskal–Wallis tests were used for continuous variables, and Student's t tests were used for categorical variables to analyze group comparisons. A p value < 0.05 was considered statistically significant if not explicitly stated. OS was defined as the time from the start of randomization to death (from any cause). Survival analyses were conducted using hazard ratios (HRs) and their corresponding 95% confidence intervals (CIs) estimated from a Cox proportional hazards model.

Results

Patient clinical characteristics

The tumor tissue samples of 155 NSCLC patients were collected retrospectively. The detailed baseline characteristics are shown in Table 1. Among all NSCLC patients, 128 patients (82.6%) had LUAD, two patients (1.3%) had LUSC, and 25 patients (16.1%) had other types of NSCLC. All patients had gene translocation events in this study. There were 84 patients (54.2%) with ALK rearrangement, 38 patients (24.5%) with RET rearrangement, and 33 patients (21.3%) with ROS1 rearrangement. The median age of this cohort was 55.0 years, ranging from 29.0 to 86.0 years. A total of 104 patients (67.1%) were females, and 51 patients (32.9%) were males. A total of 122 patients (78.7%) had no smoking history, these proportions were higher in the RET fusion-positive subgroup, which were 81.6% (Table 1). The patients in this cohort were characterized by being younger, being female, having adenocarcinoma, and having no history of smoking, consistent with the classic features of patients with ALK fusions. These data were all consistent with previous studies.[3] The clinical features of RET and ROS1 rearrangements are largely consistent with those of ALK rearrangement, so those three fusion types were subsequently combined into one category for further analysis.

TP53 and CDKN2A/B were the most common covariation genes in ALK/RET/ROS1-rearrangement samples

In this NSCLC cohort with ALK/RET/ROS1 rearrangement mutations in all samples, the most frequently observed covariations were TP53 (31%), CDKN2A/B (15%), ARID1A (7%), PTPRD (6%), SETD2 (5%), and MDM2 (5%). EGFR mutations were mutually exclusive with ROS1 fusions and had a low mutation frequency (3%) in ALK/RET fusion patients (Fig. 1A). The mutation rates of TP53 in different ALK fusion variants (V1, V2, and V3a/b) were similar. However, CDKN2A/B had the highest and most similar mutation frequency in patients with ALK V1 and V3a/b variants (Fig. 1B).

When the genomic alterations were split into SNVs and CNVs, two parts were identified. TP53 was the most frequent co-occurring gene in the SNV part (Fig. 1C). In comparison, CDKN2A/B was the most frequent co-occurring gene in the CNV part, while all variants showed loss of copy number (Fig. 1D). In detail, the top 10 co-occurring SNV alterations at all sample levels were TP53 (31.6%), ARID1A (8.4%), BRIP1 (7.7%), SETD2 (5.8%), HMCN1 (5.8%), SMAD4 (4.5%), EP300 (4.5%), ATRX (4.5%), PTEN (3.8%), and KMT2C (3.8%) (Fig. 1C). The top 10 CNVs were CDKN2A/B (loss, 13.5%), PAK7 (loss, 3.8%), PTPRD (loss, 3.8%), MDM2 (gain, 3.2%), RAC1 (gain, 2.6%), PIK3C3 (loss, 2.6%), PAX5 (loss, 2.6%), TERT (gain, 1.9%), SMAD2 (loss, 1.9%), and SDHC (gain, 1.9%) (Fig. 1D). The genes with the highest mutation frequencies of SNVs and CNVs in the cohort data were TP53 and CDKN2A/B, respectively. According to the mutation statuses of TP53 and CDKN2A/B, the patients were divided into 3 subgroups: TP53 mutation and fusion co-occurring group, CDKN2A/B variation and fusion co-occurring group, TP53/CDKN2A/B variation and fusion co-occurring group and their corresponding wild-type (WT) group.

Figure 1E and 1F show the differences in the clinicopathological characteristics of patients among the groups. The stages of cancer in the CDKN2A/B co-occurring group were significantly different from those in the WT group ($p = 0.0271$). The CDKN2A/B co-occurring group had more patients with stage IV disease (58.33% [n = 14/24] vs. 33.59% [n = 14/131]) than the CDKN2A/B WT group. In contrast, the incidence of stage I disease was significantly lower in the CDKN2A/B co-occurring group than in the CDKN2A/B WT group (0% vs. 20.61% [n = 27/131]). The same trends were also found in the TP53 or CDKN2A/B co-occurring group and TP53/CDKN2A/B WT group ($p = 0.0066$). Compared with all other stages, the proportion of patients with stage IV disease was much higher in the TP53 or CDKN2A/B co-occurring group (52.54%, n = 31/59), followed by stage III, accounting for 25.42% (n = 15/59), while the proportion of patients with stage IV disease was only 28.12% (n = 27/96) in the TP53/CDKN2A/B WT group (Fig. 1E). The sex of the patients was significantly different between the co-occurring and WT groups. The TP53 co-occurring group had more males than the TP53 WT group (56.25% [n = 27/48] vs. 22.43% [n = 24/107], $p < 0.001$), similar to the TP53 or CDKN2A/B co-occurring group compared with the control group (53.54% [n = 31/59] vs. 20.83% [n = 20/96], $p < 0.001$) (Fig. 1F).

Other clinical characteristics, including smoking, age, and cancer type, differed between the groups, as shown in Supplementary Fig. 1. These data showed that the clinical characteristics of NSCLC patients with covariation were predominantly male sex and stage IV compared with wild-type NSCLC patients. For the following reason, we combined ALK/RET/ROS1 fusions in the next analysis. The reason was that although the fusions occurred in different genes, such as RET, and ROS1, the clinical characteristics of

the included patients were well distributed and consistent with the typical clinical features of ALK fusions.

TMB and the number of neoantigens were higher in samples with TP53 or CDKN2A/B covariations

As shown in Fig. 2A, the samples in the 3 co-occurring groups had higher TMB than the samples in their corresponding WT groups ($p < 0.001$, $p = 0.017$, and $p < 0.001$). Further analysis revealed that the number of neoantigens was higher in the TP53 co-occurring group, as well as in the TP53/CDKN2A/B co-occurring group ($p = 0.014$ and $p = 0.0032$). The CDKN2A/B co-occurring group also had more neoantigens, although the difference was not statistically significant ($p = 0.31$) (Fig. 2B). Even in the HLA-A and HLA-B subgroups, there were no differences between the co-occurring and WT groups, and HLA-A*03 was a prevalent HLA type present in those groups.

TP53 or CDKN2A/B covariations were associated with an immune microenvironment characterized by high PD-L1 expression and low CD8 $^{+}$ TIL infiltration

A previous study reported that TP53/ALK comutation led to a poorer prognosis.[8] To investigate the possible reasons for this phenomenon, fluorescent mIHC with classic immune markers (CD8, CD68, PD-1, and PD-L1) was performed on 50 samples from 155 NSCLC patients harboring ALK/RET/ROS1 rearrangements, and then the differences in TIL infiltration levels were analyzed. Representative images of classic markers on tumor tissues from patient A (co-occurring group) and patient B (WT group) are shown in Fig. 3A. The lower image shows the fluorescence map of the double marker (CD8&PD-1 and CD8&PD-L1) field of view on the mIHC technology platform. The percentage of all markers was calculated separately from the tumor area, stromal area and all areas of tumor tissue. The results of these three kinds of areas were obtained separately, and the p values are presented in Supplementary Table 1.

We compared the expression levels of classic markers of the immune microenvironment in 3 regions (tumor, stroma, and all regions) in the TP53/CDKN2A/B co-occurring and WT groups. The co-occurring group had significantly less infiltration of $CD8^{+}$ ($p = 0.043$), $CD8^{+}PD\text{-}1^{-}$ ($p = 0.029$), and $CD8^{+}PD\text{-}L1^{-}$ ($p = 0.025$) TILs than the WT group (Fig. 3B). In stromal areas, the level of $CD8^{+}PD\text{-}L1^{+}$ cells was significantly increased in the covariation group compared with the WT group ($p = 0.021$). There were slightly higher trends of $CD8^{+}$, $CD68^{+}$, $CD8^{+}PD1^{-}$, and $CD68^{+}PD\text{-}L1^{-}$ infiltration in the covariation group (Fig. 3C). In the total areas, none of the markers except PD-L1 showed statistically significant differences between the two groups, and only some markers, such as $CD8^{+}$ and $CD8^{+}PD\text{-}L1^{-}$, showed a decreasing trend in the covariation group (Fig. 3D). For the comparison of the TP53 and CDKN2A/B co-occurring groups with the WT group, similar trends were also found (Supplementary Fig. 2).

Notably, the level of PD-L1$^+$ cells was higher in the covariation group than in the WT group in tumor areas ($p = 0.00038$), stromal areas ($p = 0.0016$), and total areas ($p = 0.00064$) (Fig. 3E). To reverse verify PD-L1$^+$ expression in the two groups, the expression level of PD-L1 in three different regions of the two groups was divided into high expression and low expression groups according to a 5% threshold. The results confirmed that the percentage of samples with TP53/CDKN2A/B covariations was significantly higher in the PD-L1 high expression group than in the PD-L1 low expression group in tumor areas ($p < 0.001$), stromal areas ($p = 0.04$), and total areas ($p = 0.003$) (Fig. 3F).

Overall, these results indicated that patients with co-occurring TP53/CDKN2A/B and ALK/RET/ROS1 rearrangements had an immunosuppressive microenvironment, including elevated PD-L1 expression levels and reduced overall CD8 + TILs, compared to those without co-occurring TP53/CDKN2A/B and ALK/RET/ROS1 rearrangements.

Validation of poor prognosis in patients with covariation in the TCGA NSCLC cohorts

In NSCLC patients harboring ALK/RET/ROS1 rearrangements, the above results provide important insights into the differences in prognosis between the co-occurring groups and the WT groups. Since the covariation group had higher TMB and PD-L1 expression but less CD8$^+$ TIL infiltration, we predicted a poorer prognosis in this group of patients. To validate our hypothesis, we explored the genomic co-occurring status in the LUSC and LUAD cohorts from the TCGA database. The clinical baseline characteristics included the baseline age, sex, type of cancer, stage, and smoking history. Among all 340 patients, 64.6% (n = 219) were female, and 35.6% (n = 121) were male. The median age at baseline was 60.9 years, and the age range was 16–90 years (Supplementary Table 2). The patients with co-occurrence in TCGA were characterized as young and female with adenocarcinoma and no history of smoking, which is consistent with the characteristics of our study cohort.

In NSCLC patients with ALK/RET/ROS1 rearrangements from the TCGA cohort (Fig. 4A), the top 5 mutated genes were CDKN2A/B (24%), TP53 (16%), MDM2 (8%), MYC (7%), and SETD2 (7%). As with the results of our cohort, in patients with covariation, the TMBs were significantly higher than in patients without covariation ($p < 0.001$, $p = 0.0018$, and $p < 0.001$) (Fig. 4B). The prognostic analysis showed that, regardless of whether it was the TP53 comutation group, the CDKN2A/B covariation group, or the TP53/CDKN2A/B covariation group, the OS of these three groups was shorter than that of their control groups (WT groups) ($p < 0.001$, HR = 2.53, 95% CI = 1.59–4.04; $p = 0.0625$, HR = 1.54, 95% CI = 0.97–2.42; $p < 0.001$, HR = 2.21, 95% CI = 1.47–3.33).

In summary, the trends of the validation cohort were generally consistent with our datasets in terms of clinical characteristics, the genomic alteration landscape, and TMB. Furthermore, the findings in the validation cohort suggested that the group of patients harboring the co-occurring TP53/CDKN2A/B covariations and ALK/RET/ROS1 rearrangements had a worse prognosis than the group of patients without the co-occurring TP53/CDKN2A/B covariations and ALK/RET/ROS1 rearrangements.

Discussion

The frequency of covariation in NSCLC in the presence of ALK/RET/ROS1 fusions has been reported in several studies. TP53 is the most common comutated gene with EGFR, ALK, ROS1, and other genes in lung cancer, and the presence of TP53 comutation is predictive of shorter survival.[11,12] We obtained similar results. In our cohort, the top 2 covariation genes were TP53 and CDKN2A/B (Fig. 1). Nguyen et al. found that the most frequently observed significant alteration was TP53 mutation, which was more frequent in metastases in several tumor types. A possible explanation is that TP53 mutation is a later event in some of these tumor types; in others, it may simply be a hallmark of more aggressive disease. Another genomic alteration that was most often enriched in metastases included CDKN2A deletion.[13,14] Metastases have higher chromosomal instability across many tumor types. Therefore, we speculate that tumors with enriched mutations in genes such as TP53 or CDKN2A/B may have higher TMBs and neoantigen loads.[15–17] Our study validated this hypothesis. The ALK/RET/ROS1-rearranged samples with co-occurring TP53 or CDKN2A/B in our cohort had higher TMBs and more neoantigens (Fig. 2).

The covariation leads to an increase in TMB and neoantigens, and antigen-presenting cells (APCs) present more tumor antigens to $CD8^+$ cells. After $CD8^+$ cells are activated, some cytokines, such as interferon-gamma (IFN-γ), are released to regulate immune responses.[18,19] With the activation of overall immune cells in the microenvironment (mainly $CD8^+$ cells), tumor cells and the immune system start to perform immune braking actions, manifested by tumor cells expressing PD-L1 against the killing caused by immune cell activation and immune cells in the immune system (mainly cells such as CD68) expressing PD-L1 against normal tissue damage (physiological direction), hence the increase in PD-$L1^+$ tumor cells and PD-$L1^+$ immune cells in the microenvironment.[20,21] We believe that these events occurred in the tumors of the comutation group in our cohort. Our results showed that the level of PD-$L1^+$ cells in the tumors in the TP53 or CDKN2A/B covariation group was higher than that of tumors in the WT group (Fig. 3).

Studies have found that in EGFR-mutated or ALK-rearranged lung cancers, PD-L1-positive tumors have a poorer prognosis.[22] In stage III NSCLC patients treated with chemotherapy, PD-L1-positive tumors with low $CD8^+$ cell infiltration had the worst prognosis.[23] Our study found that covariation samples had not only higher PD-$L1^+$ cells but also lower infiltration of $CD8^+$ TILs. Except for PD-L1, the expression of markers in the total region did not differ significantly between groups. $CD8^+$PD-$L1^+$ in the stroma in the covariation group was higher, which indicated that $CD8^+$ T cells were exhausted in the covariation stromal area. The expression levels of $CD8^+$, $CD8^+PD1^-$, and $CD8^+$PD-$L1^-$ in the tumor areas were lower in the covariation group, further suggesting that there were fewer non-exhausted $CD8^+$ T cells in the covariation group. Together, these results indicated that the immune microenvironment was suppressed in the covariation group. Therefore, we hypothesized that patients with covariation have a worse prognosis than WT patients. To test this hypothesis, we analyzed data from the TCGA NSCLC cohorts, and the results were as expected. The prognostic analysis showed that, regardless of whether it was the TP53 comutation group, the CDKN2A/B covariation group, or the TP53/CDKN2A/B covariation group, the

overall survival of these three groups was shorter than that of their control groups (WT groups) (Fig. 4). Several studies have demonstrated that the co-occurrence of mutation and rearrangement is a poor prognostic factor, resulting in shorter PFS and OS.[11,24]

Our observations can have a meaningful impact on clinical treatment decisions. Regarding the poor prognosis of patients with co-occurrence, this observation has also been explained in the previous section in terms of genetic heterogeneity. A. Kron conducted a molecular analysis of 216 patients with ALK-positive advanced NSCLC and hypothesized that concurrent mutations might underlie differences in prognosis. The correlation between the PD-L1 expression score and TP53 mutation status was assessed in 34 ALK-positive patients in the study, and it was found that in 8 patients (23.5%), PD-L1 was expressed in more than 50% of tumor cells. PD-L1 positivity was significantly correlated with TP53 mutation. It is tempting to speculate that a higher TMB may lead to a better effect of immune checkpoint inhibitors.[24] In a case published in 2021 by Takamasa Nakasuka of PD-L1-positive lung adenocarcinoma patient with the coexistence of RET fusions and NF1/TP53 mutations, this with poor fitness status, multiple cancer-associated thrombosis and respiratory failure eventually achieved better outcomes with pembrolizumab monotherapy.[25] This finding may provide additional insight into the efficacy of pembrolizumab immunotherapy in patients with RET fusions accompanied by comutations in TP53.

In addition, there is a special case where a comutation can occur at the time of drug resistance progression, thus giving the patient more treatment options. RET fusion has been shown to be an acquired resistance mechanism against EGFR-TKIs in approximately 5% of cases in which osimertinib resistance biopsies were performed. Piotrowska and colleagues reported two patients in whom an EGFR T790M-resistant clone was successfully suppressed by osimertinib, and a RET fusion was detected when osimertinib resistance progression was again continued genetically. In this case, the combination of osimertinib and BLU-667 was well tolerated, and a rapid radiological response was seen. RET fusion may be a relevant factor in treatment selection in the event of EGFR resistance progression.[26–28]

The limitations of this research are primarily related to the limitations of the public datasets used. The conclusions of the TME were not validated accordingly when we used the data from the TCGA database. In future work, more comprehensive cohort data should be used to overcome these limitations.

Co-occurring genomics are extremely important not only for ALK-rearranged NSCLC but also for other oncogene-driven NSCLC. For example, NSCLCs with epidermal growth factor receptor (EGFR) mutations were often found to have many co-occurring genomic events, including TP53, phosphatidylinositol-4, PIK3CA, PTEN, MET, etc.[6,29] Some of these comutated genomic events, such as high levels of ERBB2 or MET amplification, can eliminate the ability to induce a response to EGFR-TKI monotherapy.[30] Future research could be extended to investigate the mechanisms of the immune microenvironment in other oncogene-driven NSCLCs.

Conclusion

Overall, the TP53 or CDKN2A/B covariation in ALK-rearranged NSCLC is associated with a high TMB, high PD-L1 expression level characterizing the TIME and poor prognosis. The differences in prognosis and the extent of benefit from therapy between patients with and without co-occurrence may be due to differences in clinical characteristics, genomic alteration characteristics, tumor mutation loads, neoantigen levels and the immune microenvironment. Anti-PD-L1 therapy for patients with such co-occurring tumors may provide better curative effects.

Declarations

Funding: This research was funded by the Zhongnan Hospital of Wuhan University Science, Technology, and Innovation Seed Fund, grant number CXPY2019088.

Conflicts of Interest: The authors declared the following potential conflicts of interest with respect to the research, authorship, and/or publication of this article: Weikang Shao, Ting Ma, Yanhui Chen and Qingyun Li are employees of Genecast Biotechnology Co., Ltd. The other authors declare that they have no competing interests.

References

1. Caccese M, Ferrara R, Pilotto S, et al. Current and developing therapies for the treatment of non-small cell lung cancer with ALK abnormalities: update and perspectives for clinical practice. 11 2016;17:2253-2266. doi:10.1080/14656566.2016.1242578
2. Zhang SS, Nagasaka M, Zhu VW, Ou SI. Going beneath the tip of the iceberg. Identifying and understanding EML4-ALK variants and TP53 mutations to optimize treatment of ALK fusion positive (ALK+) NSCLC. *Lung Cancer*. Aug 2021;158:126-136. doi:10.1016/j.lungcan.2021.06.012
3. Rikova K, Guo A, Zeng Q, et al. Global survey of phosphotyrosine signaling identifies oncogenic kinases in lung cancer. *Cell*. Dec 14 2007;131(6):1190-203. doi:10.1016/j.cell.2007.11.025
4. Gainor JF, Shaw AT. Novel targets in non-small cell lung cancer: ROS1 and RET fusions. *Oncologist*. 7 2013;18(7):865-75. doi:10.1634/theoncologist.2013-0095
5. Bergethon K, Shaw AT, Ou SHI, et al. ROS1 rearrangements define a unique molecular class of lung cancers. 3 2012;30:863-870. doi:10.1200/JCO.2011.35.6345
6. Costa DB. TP53 mutations are predictive and prognostic when co-occurring with ALK rearrangements in lung cancer. *Ann Oncol*. Oct 1 2018;29(10):2028-2030. doi:10.1093/annonc/mdy339
7. Shaw AT, Ou SH, Bang YJ, et al. Crizotinib in ROS1-rearranged non-small-cell lung cancer. *N Engl J Med*. Nov 20 2014;371(21):1963-71. doi:10.1056/NEJMoa1406766
8. Koh J, Jang JY, Keam B, et al. EML4-ALK enhances programmed cell death-ligand 1 expression in pulmonary adenocarcinoma via hypoxia-inducible factor (HIF)-1alpha and STAT3. *Oncoimmunology*. Mar 2016;5(3):e1108514. doi:10.1080/2162402X.2015.1108514

9. Ota K, Azuma K, Kawahara A, et al. Induction of PD-L1 Expression by the EML4-ALK Oncoprotein and Downstream Signaling Pathways in Non-Small Cell Lung Cancer. *Clin Cancer Res*. Sep 1 2015;21(17):4014-21. doi:10.1158/1078-0432.CCR-15-0016
10. Gainor JF, Shaw AT, Sequist LV, et al. EGFR Mutations and ALK Rearrangements Are Associated with Low Response Rates to PD-1 Pathway Blockade in Non-Small Cell Lung Cancer: A Retrospective Analysis. *Clin Cancer Res*. Sep 15 2016;22(18):4585-93. doi:10.1158/1078-0432.CCR-15-3101
11. Christopoulos P, Kirchner M, Bozorgmehr F, et al. Identification of a highly lethal V3(+) TP53(+) subset in ALK(+) lung adenocarcinoma. *Int J Cancer*. Jan 1 2019;144(1):190-199. doi:10.1002/ijc.31893
12. Lin JJ, Ritterhouse LL, Ali SM, et al. ROS1 Fusions Rarely Overlap with Other Oncogenic Drivers in Non-Small Cell Lung Cancer. *J Thorac Oncol*. May 2017;12(5):872-877. doi:10.1016/j.jtho.2017.01.004
13. Jiang J, Gu Y, Liu J, et al. Coexistence of p16/CDKN2A homozygous deletions and activating EGFR mutations in lung adenocarcinoma patients signifies a poor response to EGFR-TKIs. *Lung Cancer*. Dec 2016;102:101-107. doi:10.1016/j.lungcan.2016.10.015
14. Nguyen B, Fong C, Luthra A, et al. Genomic characterization of metastatic patterns from prospective clinical sequencing of 25,000 patients. 2021;doi:10.1101/2021.06.28.450217
15. Belinsky SAN, K.J. Palmisano, W.A. Michels, R. Saccomanno, G. Gabrielson, E. Baylin, S.B. Herman, J.G. Aberrant Methylation of p16 INK4a Is an Early Event in Lung Cancer and a Potential Biomarker for Early Diagnosis. 1998;95:11891-11896.
16. Deneka AYB, Y.Serebriiskii, I.G.Nicolas, E.Parker, M.I. Xiu, J. Korn, W.M.Demeure, M.J. Wise-Draper, T.. Association of T P53 and CDKN2A Mutation Profile with Tumor Mutation Burden in Head and Neck Cancer. 2022;28:1925-1937.
17. Alidousty C, Baar T, Martelotto LG, et al. Genetic instability and recurrent MYC amplification in ALK-translocated NSCLC: a central role of TP53 mutations. *J Pathol*. Sep 2018;246(1):67-76. doi:10.1002/path.5110
18. Tumeh PC, Harview CL, Yearley JH, et al. PD-1 blockade induces responses by inhibiting adaptive immune resistance. *Nature*. Nov 27 2014;515(7528):568-71. doi:10.1038/nature13954
19. Xu-Monette ZY, Zhang M, Li J, Young KH. PD-1/PD-L1 Blockade: Have We Found the Key to Unleash the Antitumor Immune Response? *Front Immunol*. 12 2017;8:1597. doi:10.3389/fimmu.2017.01597
20. Liu Y, Zugazagoitia J, Ahmed FS, et al. Immune Cell PD-L1 Colocalizes with Macrophages and Is Associated with Outcome in PD-1 Pathway Blockade Therapy. *Clin Cancer Res*. Feb 15 2020;26(4):970-977. doi:10.1158/1078-0432.CCR-19-1040
21. Dong ZY, Zhong WZ, Zhang XC, et al. Potential Predictive Value of TP53 and KRAS Mutation Status for Response to PD-1 Blockade Immunotherapy in Lung Adenocarcinoma. *Clin Cancer Res*. Jun 15 2017;23(12):3012-3024. doi:10.1158/1078-0432.CCR-16-2554
22. Liu SY, Dong ZY, Wu SP, et al. Clinical relevance of PD-L1 expression and CD8+ T cells infiltration in patients with EGFR-mutated and ALK-rearranged lung cancer. *Lung Cancer*. Nov 2018;125:86-92.

doi:10.1016/j.lungcan.2018.09.010

23. Tokito T, Azuma K, Kawahara A, et al. Predictive relevance of PD-L1 expression combined with CD8+ TIL density in stage III non-small cell lung cancer patients receiving concurrent chemoradiotherapy. *Eur J Cancer*. Mar 2016;55:7-14. doi:10.1016/j.ejca.2015.11.020
24. Kron A, Alidousty C, Scheffler M, et al. Impact of TP53 mutation status on systemic treatment outcome in ALK-rearranged non-small-cell lung cancer. *Ann Oncol*. Oct 1 2018;29(10):2068-2075. doi:10.1093/annonc/mdy333
25. Nakasuka T, Ohashi K, Watanabe H, et al. A case of dramatic reduction in cancer-associated thrombus following initiation of pembrolizumab in patient with a poor performance status and PD-L1(+) lung adenocarcinoma harboring CCDC6-RET fusion gene and NF1/TP53 mutations. *Lung Cancer*. Jun 2021;156:1-4. doi:10.1016/j.lungcan.2021.03.022
26. Rich TA, Reckamp KL, Chae YK, et al. Analysis of Cell-Free DNA from 32,989 Advanced Cancers Reveals Novel Co-occurring Activating RET Alterations and Oncogenic Signaling Pathway Aberrations. *Clin Cancer Res*. Oct 1 2019;25(19):5832-5842. doi:10.1158/1078-0432.CCR-18-4049
27. Klempner SJ, Bazhenova LA, Braiteh FS, et al. Emergence of RET rearrangement co-existing with activated EGFR mutation in EGFR-mutated NSCLC patients who had progressed on first- or second-generation EGFR TKI. *Lung Cancer*. Sep 2015;89(3):357-9. doi:10.1016/j.lungcan.2015.06.021
28. Piotrowska Z, Isozaki H, Lennerz JK, et al. Landscape of Acquired Resistance to Osimertinib in EGFR-Mutant NSCLC and Clinical Validation of Combined EGFR and RET Inhibition with Osimertinib and BLU-667 for Acquired RET Fusion. *Cancer Discov*. Dec 2018;8(12):1529-1539. doi:10.1158/2159-8290.CD-18-1022
29. Aisner DL, Sholl LM, Berry LD, et al. The Impact of Smoking and TP53 Mutations in Lung Adenocarcinoma Patients with Targetable Mutations-The Lung Cancer Mutation Consortium (LCMC2). *Clin Cancer Res*. Mar 1 2018;24(5):1038-1047. doi:10.1158/1078-0432.CCR-17-2289
30. Carney BJ, Rangachari D, VanderLaan PA, et al. De novo ERBB2 amplification causing intrinsic resistance to erlotinib in EGFR-L858R mutated TKI-naive lung adenocarcinoma. *Lung Cancer*. Dec 2017;114:108-110. doi:10.1016/j.lungcan.2017.08.018

Table

Table 1 is available in the Supplementary Files section.

Figures

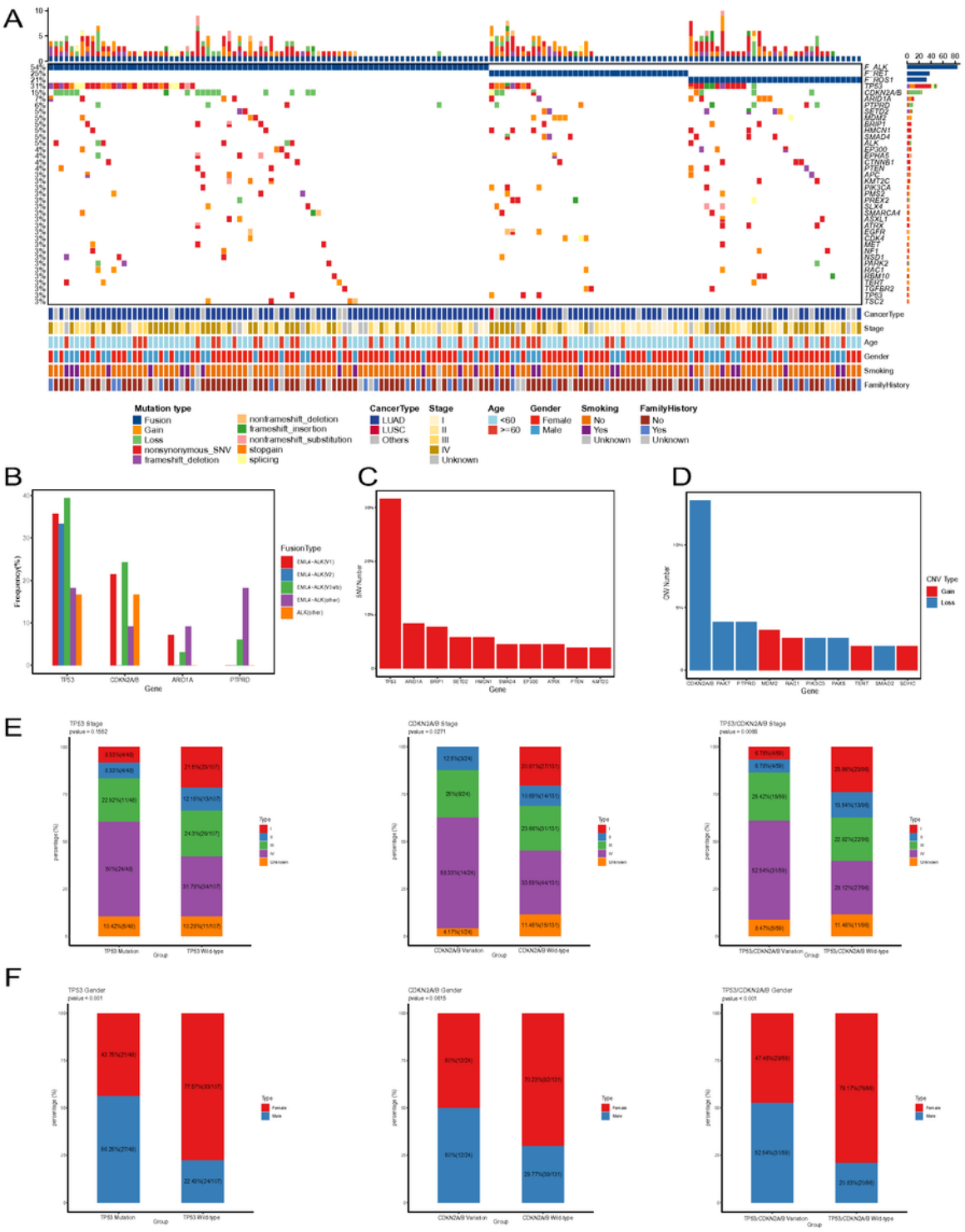

Figure 1

Summary of ALK/RET/ROS1 rearrangements and covariations in this cohort. *(A) Landscape of genomicalterations in all samples. Different colors represent different mutation types. (B) The mutation rates of TP53, CDKN2A/B, ARID1A, and PTPRD in samples with different variants of ALK fusion. Different colors represent different variants. (C) The top 10 co-occurring SNV genes. (D) The top 10 co-occurring CNV genes and their variation types. (E-F) Clinicopathologic characteristics of cancer stages (E) and sex*

(F) in the TP53 co-occurring and TP53 WT groups, CDKN2A/B co-occurring and CDKN2A/B WT groups, and TP53/CDKN2A/B co-occurring and TP53/CDKN2A/B WT groups.

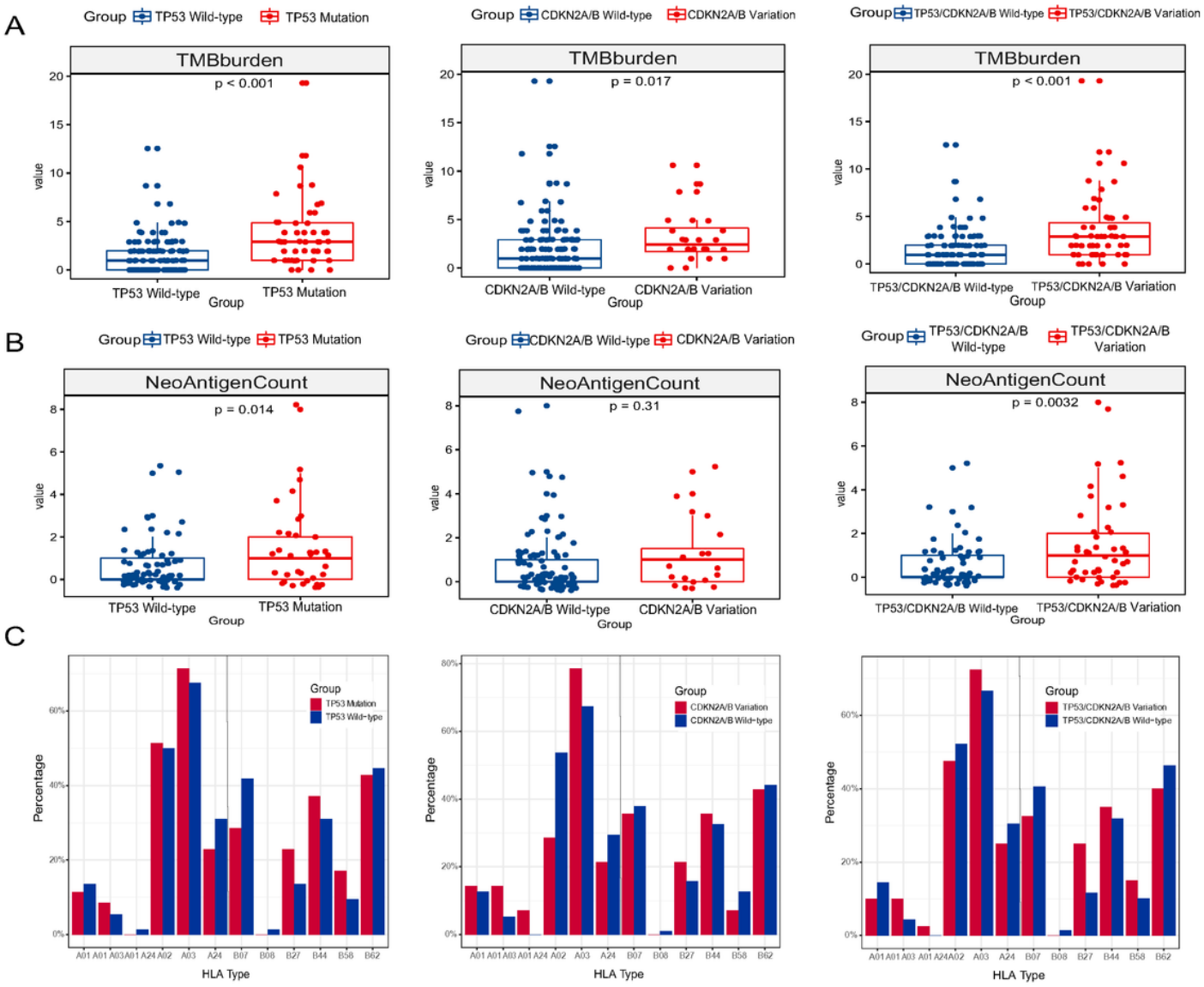

Figure 2

Differences in the TMB, neoantigen counts, and HLA types between the co-occurring groups and WT groups. *(A-B) Box plots showing the differences in TMB (A) and neoantigen counts (B) between the co-occurring groups and the WT groups. (C) Bar plots showing the percentage of HLA types among the co-occurring groups and WT groups. Red indicates the TP53, CDKN2A/B, and TP53/CDKN2A/B co-occurring groups. Blue indicates the TP53, CDKN2A/B, and TP53/CDKN2A/B WT groups.*

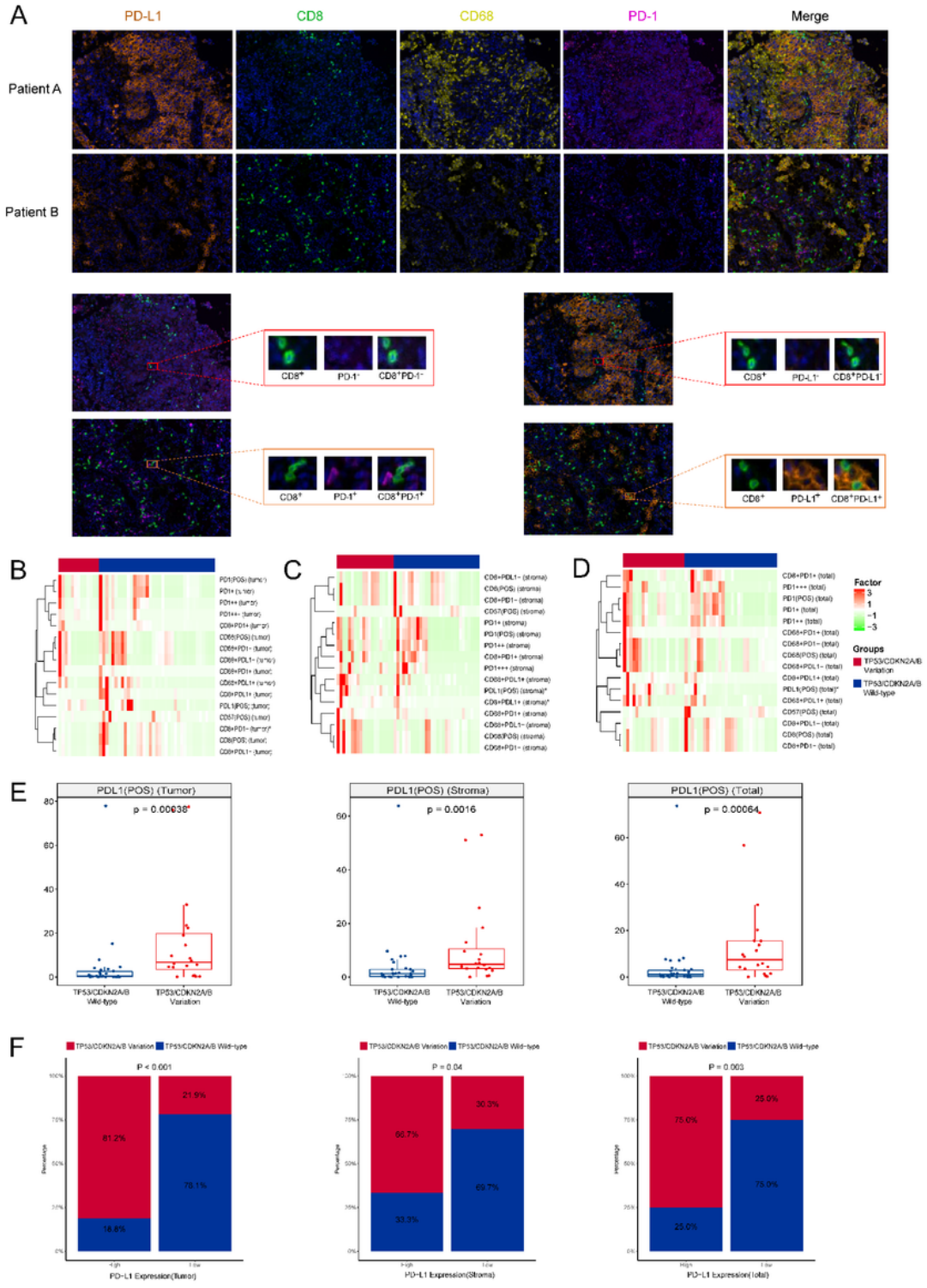

Figure 3

Comparison of PD-L1 expression and TIL infiltration in all samples without/with TP53 or CDKN2A alterations. (A) Representative images of mIHC staining for PD-L1, CD8, CD68, and PD-1. Patient A: co-occurring group; patient B: wild-type group. The lower plots show the fluorescence maps of $CD8^{+}PD\text{-}1^{-}$ and $CD8^{+}PD\text{-}L1^{-}$ cells. (B-D) Heatmaps showing the differences in the expression level of each type of immune cell between the co-occurring groups and WT groups in tumor areas (B), stromal areas (C), and

all areas (D). The values are scaled across each marker (rows) and are represented by the Z score, with red and green representing high and low relative percentages of expression, respectively. (E) The level of PD-L1^{+} cells between the co-occurring groups and WT groups in tumor areas, stromal areas, and all areas. (F) Histogram showing the reverse validation of PD-L1 expression in tumor areas, stromal areas, and all areas in the two groups.

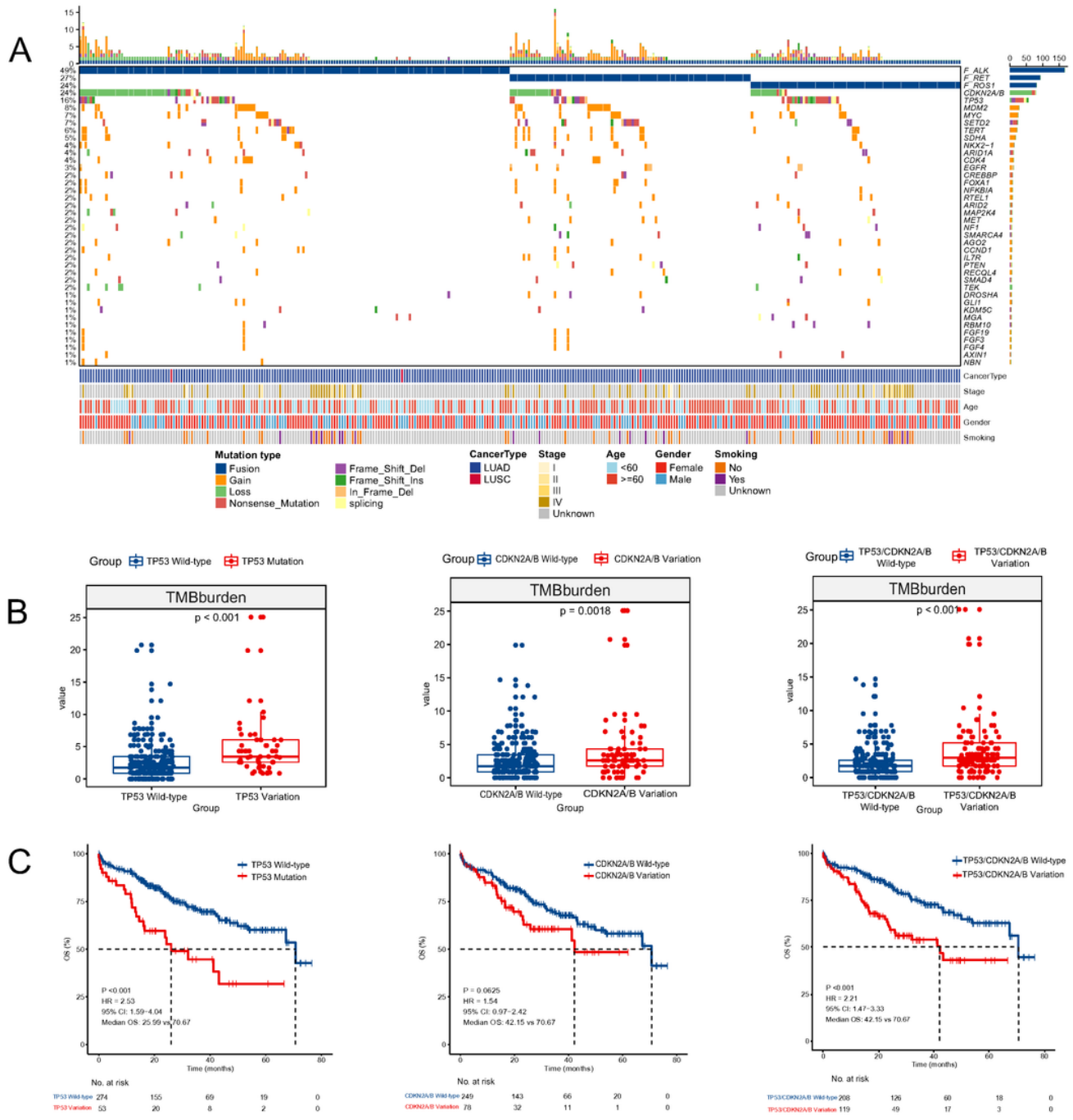

Figure 4

Landscape of genomic variation signatures and prognostic analysis in patients from the TCGA NSCLC cohorts. *(A) Landscape of the genomicalterations of the TCGA cohorts. Different colors represent*

different variation types. (B) The differences in TMB between the co-occurring mutation groups and the WT groups. (C) Kaplan–Meier survival curves of overall survival between the groups with and without covariation.

Supplementary Files

This is a list of supplementary files associated with this preprint. Click to download.

- SupplementaryFile.docx
- Table1.xlsx